Temperature, Current, and Voltage Dependences of Junction Failure in PIN Photodiodes

Sahnggi Park, Eundeok Sim, Jeong-Woo Park, Jae-Sik Sim, Hyun-Woo Song, Su Hwan Oh, and Yongsoon Baek

A PIN photodiode having a low dark current of 1.35 nA and a high external quantum efficiency of 95.3% fabricated for a passive optical network receiver. As the current was increased under a high voltage of 38 V and a temperature of 190°C, it was observed that there is a threshold current at 11 mA which induces a junction failure. Experimental data suggest that the junction failure occurs due to the crystal breaking at the end facet as a result of thermal heat or energetic carriers. This threshold behavior of junction failure is a valuable observation for the safe treatment of photodiodes. As long as the current is limited below the threshold currents, we have not observed failure events of our photodiodes.

Keywords: Photodiodes, detectors, reliability, junction failure, dark current.

Manuscript received Dec. 19, 2005; revised May 16, 2006.

This work was supported by the Ministry of Information and Communication of the Korean Government.

Sahnggi Park (phone: + 82 42 860 1655, email: sahnggi@etri.re.kr), Eundeok Sim (email: sed63252@etri.re.kr), Jeong-Woo Park (email: pjw21@etri.re.kr), Jae-Sik Sim (email: jssim@etri.re.kr), Hyun-Woo Song (email: hwsong@etri.re.kr), Su Hwan Oh (email: osh@etri.re.kr), and Yongsoon Baek (email: yongb@etri.re.kr) are with IT Convergence & Components Laboratory, ETRI, Daejeon, Korea.

I. Introduction

The reliability of InP/InGaAs photodiode detectors has been studied for more than two decades [1], [2] and failure modes have been analyzed by several groups of researchers [3]-[14]. The failure criteria of photodiode detectors have been based on dark current deteriorations after specific hours of accelerated degradation of the detectors. The analysis of failure modes aims to find the source of dark current that is possibly aggravated by imposed stresses, high temperature, high reverse-bias voltage, and high relative humidity.

From the failure mode analysis of planar zinc-diffused InGaAs/InP PIN photodiodes, Chin and others [3] reported that the pinholes in the SiN_x diffusion mask, at less than 5 μm distance from the edge of the p-n junction, are the major sources of microplasmas in the devices with low leakage current. Unintentional zinc diffusion through the pinholes produces a p-region of a small dimension that locally increases the electric field to enhance the leakage current [3], [4].

From a thermal run-away analysis for velocity-matched distributed photodetectors (PDs), Nespola and others [5] reported that the thermal run-away can be assumed as a fair indicator of potential catastrophic failure for high-power detectors. Diffusion of gold into a semiconductor was experimentally shown to be a major cause of catastrophic failure in actual devices [5]-[7].

From the dark current analysis, Williams and others [8] and Islam and others [9] reported that thermally activated dark current can cause PD failure when the increase of dark current causes an additional increase in the diode temperature, resulting in additional dark current, and this positive feedback process continues until the PDs fail [8]-[11].

Failure modes attributed to hot holes or mobile ions have been reported by several groups of researchers. Mawatari and others [12] and Kuhara and others [13] concluded that the deterioration of a p-n junction on a cleaved facet of failed planar waveguide photodiodes was caused by hot hole injection or mobile ion accumulation in the passivated film [12], [13]. Sudo and others [14] proposed a surface degradation mechanism, positive charge accumulation in the passivation film of avalanche photodiodes, followed by local avalanche multiplication at the guard-ring periphery [14].

The humidity dependence of failure has been analyzed by Osenbach and others [15], who proposed that ingress of moisture to the InP surface gives off hydrogen at the p-contact region of the device. Under negative bias, In and P react with the hydrogen to form gaseous InH and PH_3. This leads to semiconductor erosion and subsequently device failure [15], [16]. Although there are many other articles and letters discussing the failure mode of detectors, most of them fall into the following four categories: localized increase of the electric field; contamination of metal contact; deterioration due to mobile ions, hot holes, or thermal run-away; and high relative humidity-induced erosion.

Reverse-bias voltages in most reliability tests are just below the diode breakdown voltage at which specific amounts of current may flow through the junction to degrade the junction characteristics. Although the diodes are regarded as having failed by the dark current criteria, the diodes are still far from complete failure by junction breakage where the current-voltage (I-V) curves are abnormal. As the reverse bias increases further beyond the diode breakdown voltage, the diode reaches the point where junction characteristics are completely distorted as I-V curves are observed. The voltage, current, and temperature behaviors of photodiodes near junction failure have not been thoroughly studied except crystal breakage due to joule heating.

In this paper, we report a threshold characteristic of junction failure as the voltage, current, and temperatures are increased until junction failure. Two failure modes are proposed, in relation to joule heating and energized carriers induced by the locally increased electric field. It is also shown that the diodes are quite safe as long as the variables of voltage, current, and temperature are kept below the threshold for some minutes.

II. Design and Fabrication

To investigate photodiode behavior near junction failure, it is important to design the epitaxial structure of photodiodes which may sustain at a large leakage current under high reverse vias near the junction failure. The cross-sectional design shown in Fig. 1 was proved to match with this experiment. The layers were grown by metal organic vapor phase epitaxy on a (100)-oriented n-InP substrate. The side-illuminated PIN photodiode consists of a 20 μm-wide multimode graded index waveguide that has a 100 μm or 200 μm length. The core layers of the waveguide consist of a 0.2 μm-thick undoped $In_{0.53}Ga_{0.47}As$ active layer, n- or p-doped InGaAsP quaternary layers, and index-diluted layers. The quaternary layers have a band gap of 1.24 μm and a thickness of 0.2 μm, or a band gap of 1.1 μm and a thickness of 0.5 μm. The index-diluted layers consist of seven pairs of 100 nm-thick InP layers and 50 nm-thick InGaAsP layers (a band gap of 1.1 μm) [17]. The index-diluted layer has an effective index of 3.22 at the wavelength of 1.55 μm. The doping concentration is $5\times10^{17}/cm^3$ for p-doping and $1\times10^{18}/cm^3$ for n-doping. The cladding layers consist of an n-doped substrate and a p-doped, 2 μm-thick InP layer. The waveguide is designed to give an optimum coupling efficiency with a flat-cut standard single mode fiber or a planar light wave circuit (PLC) platform which can be used in the Ethernet-passive optical network (E-PON) or wavelength division

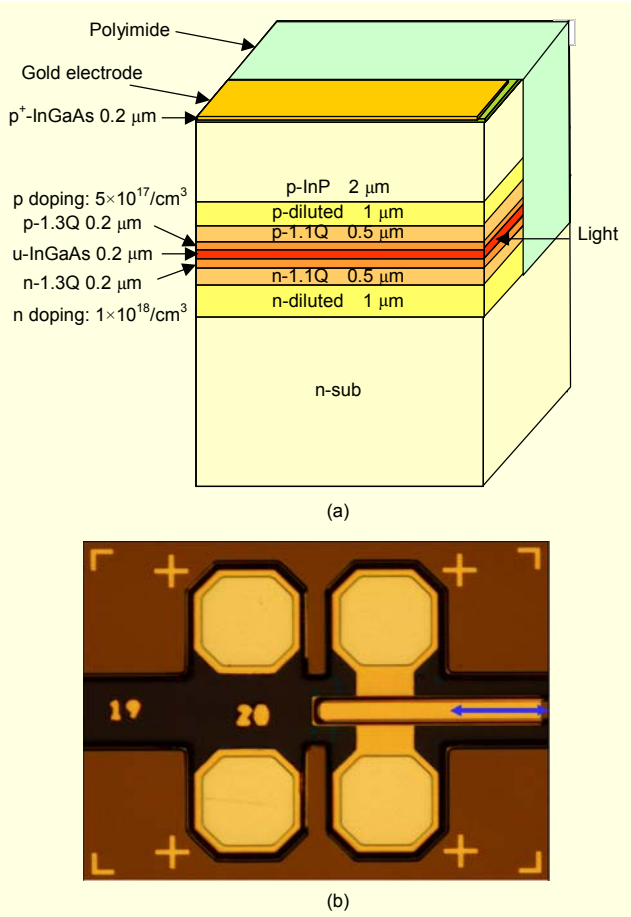

Fig. 1. (a) A schematic view of the photodiode structure and (b) a microscopic image of a photodiode, where the arrow represents the cross-sectional direction of the schematic view drawn in (a).

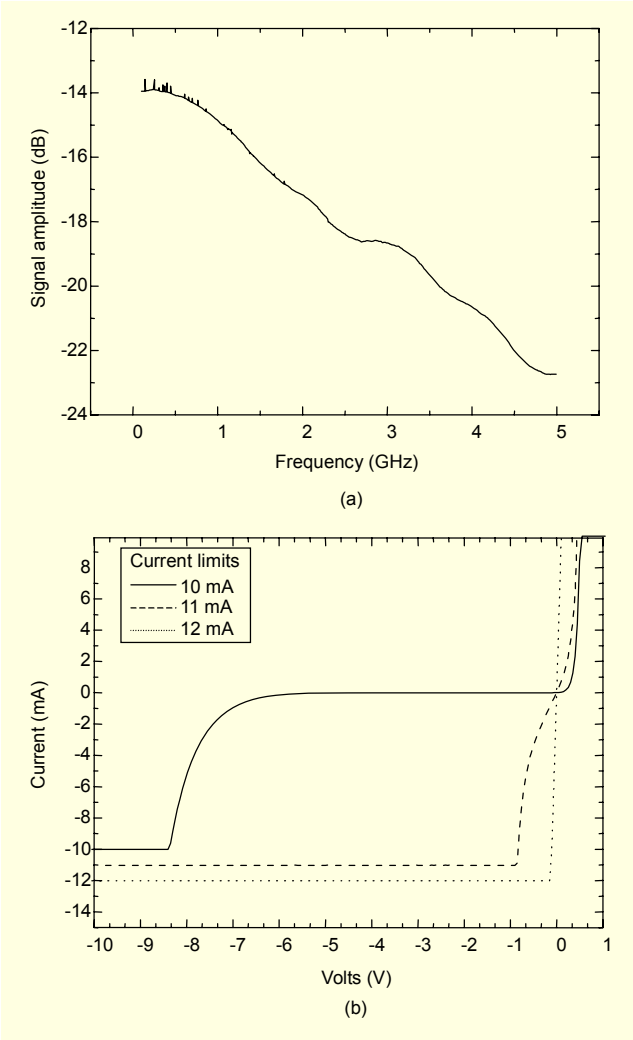

Fig. 2. (a) Signal amplitude as a function of signal frequency to measure the bandwidth of photodiode and (b) current-voltage characteristics of the photodiodes with different current limits (bias voltage from -40V to 1V).

multiplexing passive optical network (WDM-PON) receiver [18], [19].

The waveguide of the photodiode was patterned using photolithography and a 4 μm-deep dry etch, followed by a wet etch that can ease the roughness of the dry-etched surface. A polyimide layer was spin-coated and patterned to provide the lateral confinement and the electrical isolation. After p-contact metal was established, the top surface of the photodiode was passivated by a SiN_x film at 265°C.

The polyimide layer was highly resistant to the dark current of 1.35 nA which was obtained by averaging the absolute values of dark current between -3.5V and -0.1V in the I-V curve. The dark current was measured at 23°C with the area of 20×200 μm^2 before dielectric-coating at the end facet. A completed photodiode chip showed high electrical and optical characteristics. The highest responsivity at 1550 nm was 0.91 A/W with a flat-cut fiber and 1.19 A/W with a lensed fiber of which the external quantum efficiency is 95.3%. This may be compared with 95%, the highest value from our extended search reported by Takeuchi and others in 1998 [20]. The bandwidth measurement is shown in Fig. 2(a), being the 3 dB bandwidth of 1.7 GHz with the 100 μm-long waveguide, which is higher than our targeted minimum value, 1.25 GHz for the PON receiver. The current and voltage characteristics are shown in Fig. 2(b). The breakdown voltage is 7 V at 250°C. This low breakdown voltage is useful for studying the junction failure as described below. The curves were obtained with the bias voltage from -40 V to 1 V and the current limits, 10 mA for the solid line, 11 mA for the dashed line, and 12 mA for the dotted line, where the current limit is the highest allowed current set in the measurement instrument, HP4145b. The photodiode shows a normal I-V curve for the current limit of 10 mA. With 11 mA, however, the normal I-V curve starts to be destroyed, indicating a junction failure. The junction is completely destroyed at 12 mA indicating a short between two electrodes.

The junction failures as functions of voltage and temperature are shown in Fig. 3. To obtain the graphs in Fig. 3, 100 chips having low dark currents were held on a hot plate, where probe tips were contacted on the pads of the chips while changing the temperature of the hot plate. The I-V curves with different current limits were obtained using HP4145b. Figure 3(a) shows the current limits for junction failure as a function of the highest reverse bias at 250°C. Figure 3(b) shows the current limits for junction failure as a function of temperature, where the junction failure was decided by measuring I-V curves changed from -40 V to 1V at each temperature. From the figures, we can summarize the features of the two graphs as follows:

1) There are current thresholds of which uncertainties are very small (less than ±0.5 mA) above 38 V in (a) and 190°C in (b), while the uncertainties are larger than ±1 mA below 38 V in (a) and below 190°C in (b).
2) The current threshold of 11 mA above 38 V in (a) and 190°C in (b) is constant until 43 V, the voltage allowed by the system HP4145b at the temperature of 250°C.
3) The current thresholds have very large uncertainties (larger than ±5 mA) near the values 38 V in (a) and 190°C in (b).
4) The two graphs show similarly shaped curves. These features are interesting for the safe treatment of photodiodes as well as the theoretical approach to the junction failures. In our study, this threshold behavior of junction failure of photodiodes is observed and discussed for the first time to our knowledge.

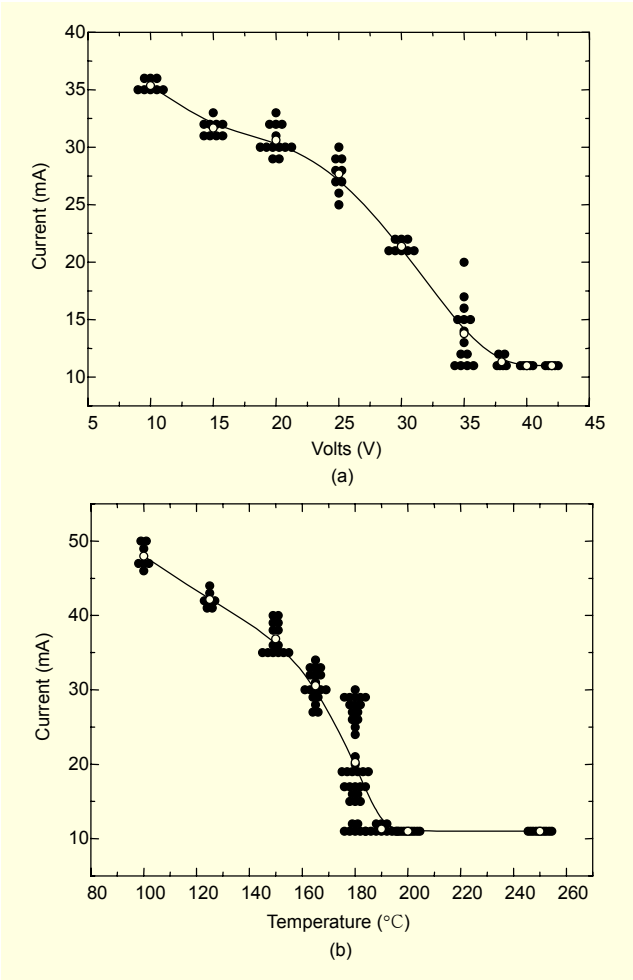

Fig. 3. Current limits for junction failure (a) as a function of the highest reverse bias at 250°C and (b) as a function of temperature with the highest reverse bias of 40 V. Blank circles represent average values of the data points.

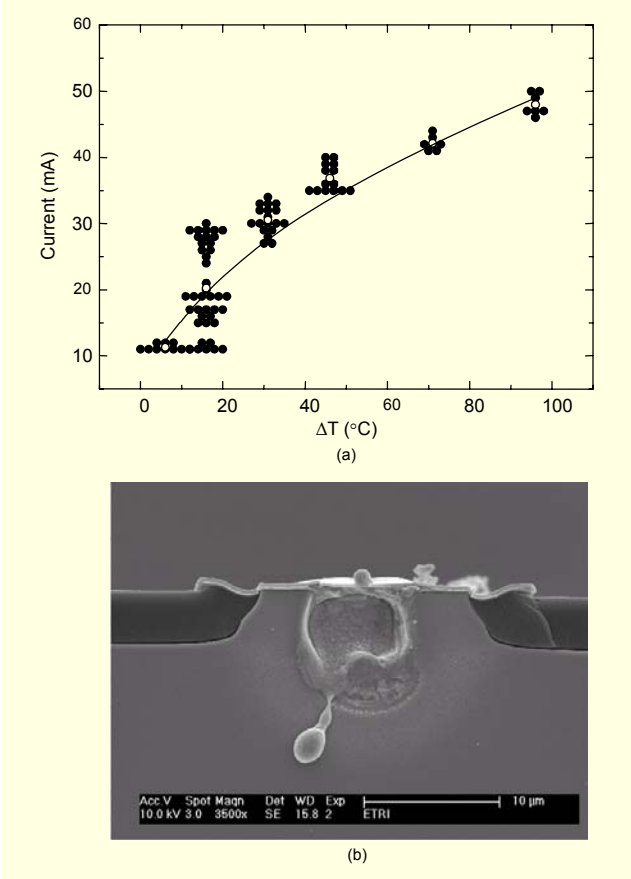

Fig. 4. (a) A current square-function fits to the part of thermal heating and (b) a SEM picture showing a crystal break at the end facet of a photodiode.

III. Discussion and Conclusion

A possible explanation for these features of junction failure is the following. Below the voltage of 38 V as shown in Fig. 3(a) and the temperature of 190°C as shown in Fig. 3(b), junction failure occurs due to thermal heat. Thermal heat has a linear relation with temperature and carrier energy, $\Delta H \propto \Delta T \propto e\Delta V$, and thermal heat is proportional to the current square, $\Delta H \propto I^2$. Consequently, the temperature and the carrier energy are proportional to the current square. A part of Fig. 3(b) from 100°C to 190°C is plotted in Fig. 4(a) in such a way that the horizontal axis represents a temperature difference, ΔT=190°C-T. The solid line is a fit with a function, $\Delta T = I^2/25$. The experimental points are in good agreement with the function where 1/25 is an arbitrary fitting constant. Although it is not represented here, the voltage curve also is in good agreement with the same function having a different constant. From this agreement, we infer that the junction failure below 38 V shown in Fig. 3(a) and 190°C shown in Fig. 3(b) is due to thermal heat.

Above 38 V in Fig. 3(a) and 190°C in Fig. 3(b), we have a constant current, 11 mA for the junction to fail. We suppose that the junction failure is due to the energetic carriers. There are a minimum number of carriers corresponding to 11 mA to break a specific part of the crystal structure. At a high voltage and temperature, each carrier transfers its energy to a branch of the crystal bond causing the branch to break. Figure 4(b) is an image taken with a scanning electron microscope (SEM) showing a crystal break at the end facet of a photodiode, where the local electric field is the highest. After removing the end facet of a junction-failed photodiode, we measured a normal I-V curve. We may conclude that the junction failure in our photodiode occurred due to the crystal break at the end facet caused by thermal heat or energetic carriers. Large uncertainties (larger than ± 5mA) near the values of 38 V in Fig. 3(a) and 190°C in Fig. 3(b) suggest that the failure modes, thermal heat, and energetic carriers co-exist near the values 38 V and 190°C.

As long as the current is limited below the threshold currents, for example, 11 mA at 40 V and 250°C, the photodiodes are very safe. We compared the dark currents of the treated and untreated chips under the conditions of 9 mA, 40 V, and 250°C which are just below the threshold of junction failure. The dark current averages of 10 chips are 1.352 nA with untreated chips and 1.373 nA with treated chips. The dark currents are effectively the same because the difference is much smaller than the measurement variation standard deviation (SD) which is 0.4 nA. The responsivity and I-V curves were also indistinguishable. From this measurement, we may conclude that the photodiodes are safe as long as the currents are kept below the threshold for some minutes.

In conclusion, a PIN photodiode having a low dark current of 1.35 nA and a high external quantum efficiency of 95.3% was fabricated for a PON receiver. As the current limit was increased at high voltage and temperature, a threshold current for junction failure was observed. The threshold current showed different behaviors between, above, and below the reverse bias of 38 V and the temperature of 190°C. Experimental data suggest that the junction failure in our photodiode occurs due to the crystal break at the end facet caused by thermal heat or energetic carriers. As long as the current is limited below the threshold current, we observed that the photodiodes are safe.

Acknowledgement

The authors wish to acknowledge their colleagues in Electronics and Telecommunications Research Institute for fruitful discussions.

References

[1] S.R. Forrest, R.F. Leheny, R.E. Nahory, and M.A. Pollack, "$In_{0.53}Ga_{0.47}As$ Photodiodes with Dark Current Limited by Generation-Recombination and Tunneling," *Appl. Phys. Lett*., vol. 37, 1980, pp. 322-325.

[2] T.P. Lee and C.A. Burrus, "Dark Current and Breakdown Characteristics of Dislocation-Free InP Photodiodes," *Appl. Phys. Lett*., vol. 36, 1980, pp. 587-589.

[3] A.K. Chin, F.S. Chen, and F. Ermanis, "Failure Mode Analysis of Planar Zinc Diffused $In_{0.53}Ga_{0.47}As$ PIN Photodiodes,'' J. *Appl. Phys*., vol. 55, 1984, pp. 1596-1606.

[4] R.H. Saul and F.S. Chen, "Reliability Assurance for Devices with a Sudden Failure Characteristic," *IEEE Electron Device Lett*., vol. ELD-4, 1983, pp. 467-468.

[5] A. Nespola, T. Chau, M.C. Wu, and G. Ghione, "Analysis of Failure Mechanism in Velocity-Matched Distributed Photodiodes," *IEE Pro. Optoelectron*., vol. 146, 1999, pp. 25-30.

[6] M.S. Islam, A. Nespola, M. Yeahia, M.C. Wu, D.L. Sivco, and A.Y. Cho, "Correlation Between the Failure Mechanism and Dark Currents of High Power Photodetectors," *LEOS 2000 Annual Meeting* (Cat. No.00CH37080), vol. 1, 2000, pp. 82-83.

[7] Y. Tashiro, K. Taguchi, Y. Sugimoto, T. Torikai, and K. Nishida, "Degradation Modes in Planar Structure $In_{0.53}Ga_{0.47}As$ Photodetectors," *J. Lightwave Technol*., vol. LT-1, 1983, pp. 269-272.

[8] K.J. Williams and R.D. Esman, "Design Considerations for High-Current Photodetectors," *J. Lightwave Technol*., vol. 17, 1999, pp. 1443-1454.

[9] M.S. Islam, T. Jung, T. Itoh, M.C. Wu, A. Nespola, D.L. Sivco, and A.Y. Cho, "High Power and Highly Linear Monolithically Integrated Distributed Balanced Photodectectors," *J. Lightwave Technol*. vol. 20, 2002, pp. 285-295.

[10] J.S. Paslaski, P.C. Chen, C.M. Gee, and N. Bar-Chaim, "High Power Microwave Photodiode for Improving Performance of RF Fiber Optic Links," *Proc. SPIE, Photon. Radio Freq*., vol. 2844, 1996, Denver, CO, pp. 110-119.

[11] M.S. Islam and M.C. Wu, "Recent Advances and Future Prospects in High-Speed and High-Saturation Current Photodetectors," *Proc. SPIE*, vol. 5246, 2003, pp. 448-457.

[12] H. Mawatari, M. Fukuda, K. Kato, T. Takeshita, M. Yada, A. Kozen, and H. Toba, "Reliability of Planar Waveguide Photodiodes for Optical Subscriber Systems," *J. Lightwave Technol*., vol. 16, 1998, pp. 2428-2434.

[13] Y. Kuhara, H. Terauchi, and H. Nishizawa, "Reliability of InGaAs/InP Long-Wavelength PIN Photodiodes Passivated with Polyimide Thin Film," *J. Lightwave Technol.,* vol. LT-4, 1986, pp. 933-937.

[14] H. Sudo and M. Suzuki, "Surface Degradation Mechanism of InP/InGaAs APD's," *J. Lightwave Technol*., vol. 6, 1988, pp. 1496-1501.

[15] J.W. Osenbach and T.L. Evanosky, "Temperature-Humidity-Bias Behavior and Acceleration Model for InP Planar PIN Photodiodes," *J. Lightwave Technol*., vol. 14, 1996, pp. 1865-1881.

[16] R.B. Comizzoli, J.W. Osenbach, G.R. Crane, G.A. Peins, D.J. Siconolfi, O.G. Lorimor, and C.C. Chang, "Failure Mechanism of Avalanche Photodiodes in the Presence of Water Vapor," *J. Lightwave Technol*., vol. 19, 2001, pp. 252-265.

[17] S. Demiguel, N. Li, X. Li, X. Zheng, J. Kim, J.C. Campbell, H. Lu, and A. Anselm, "Very High-Responsivity Evanescently Coupled Photodiodes Integrating a Short Planar Multimode Waveguide for High-Speed Applications," *IEEE Photon. Technol. Lett*., vol. 15, 2003, pp. 1761-1763.

[18] S.H. Oh, H.S. Ko, K.S. Kim, J.M. Lee, C.W. Lee, O.K. Kwon, S.G. Park, and M.H. Park, "Fabrication of Butt-Coupled SGDBR Laser Integrated with Semiconductor Optical Amplifier Having a Lateral Tapered Waveguide," *ETRI Journal*, vol. 27, 2005, pp.

551-556.

[19] Y.H. Kwon, J.S. Choe, J.H. Kim, K.S. Kim, K.S. Choi, B.S. Choi, and H.G. Yun, "Fabrication of 40Gb/s Front-End Optical Receivers Using Spot-Size Converter Integrated Waveguide Photodiodes," *ETRI Journal*, vol. 27, 2005, pp. 484-490.

[20] T. Takeuchi, T. Nakata, M. Tachigori, K. Makita, and K. Taguchi, "Design and Fabrication of a Waveguide Photodiode for 1.55-μm Band Access Receivers," *10th Intern. Conf. on Indium Phosphide and Related Materials*, TuP-48, 1998, pp. 262-265.

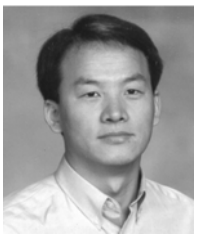

Sahnggi Park received a PhD degree in optics from the University of Arizona, US in 1999, and both MS and BS degrees in physics from Kyungpook National University, Korea, in 1988 and 1986. Since March 2001, he has been a Senior Research Engineer with Electronics & Telecommunication Research Institute (ETRI), Korea. From January 2000 to February 2001, he was a Senior Research Engineer in Samsung Electronics Co. His research projects have been in the fields of semiconductor lasers and detectors, optical fibers and communication devices, and DRAM and memory devices at Samsung Electronics Co.

Eundeok Sim received his BS, MS, and PhD degrees in physics from Yonsei University, Korea, in 1994, 1996, 2001, respectively. He joined the Basic Research Laboratory of ETRI, Korea in 2001 and has worked since then on InP-based optoelectronic devices.

Jeong-Woo Park received the BS, MS and PhD degree from Seoul National University, Korea, in 1992, 1994, and 1999, respectively. He was a Senior Engineer in the memory department of Samsung, Korea, where he worked on digital and analog circuit design, from 1999 to 2001. He joined the Optical Communication Devices Department of Electronics and Telecommunications Research Institute (ETRI), Korea, as a Senior Engineer, in 2001. He is currently with the Optical Devices Department, ETRI, where he works on silicon photonics. His research interests include silicon based optical devices such as silicon based light sources, photodiodes, modulators, and MUXs/DEMUXs.

Jae-Sik Sim received the BE and ME degrees from Sung Kyun Kwan University, Suwon, Korea, in 1999 and 2001, respectively. He joined the Integrated Optical Source Team of ETRI, Korea, in 2001, and has been engaged in the research and development of spot-size converter integrated lasers and integrated WDM optical transmitter modules. His research interests include the design and fabrication of the 60 GHz analog optical transceiver module for RF/optic conversion.

Hyun-Woo Song received the BSc in physics in 1990 from Kyungpook National University, Daegu, Korea. He received the PhD in semiconductor optics in 1999 from KAIST, Daejeon, Korea. From 1999, he has worked in the Optical Devices Group, ETRI, Korea. His research interests are in semiconductor optical sources for optical communication, such as diode lasers and vertical-cavity surface-emitting lasers.

Su Hwan Oh received the BS, MS, and PhD degrees in electronics and communications engineering from Korea Maritime University in 1991, 1995, and 1999. During his PhD work, he studied GaInAsP/InP long wavelength semiconductor lasers. From 1999 to 2000, he worked on the development of GaN devices using MBE systems at the Department of Electrical and Electronics Engineering from Sophia University in Japan. In 2000, he joined the Optical Communication Devices Department of Electronics and Telecommunications Research Institute (ETRI), Korea, where he was engaged in research on the development of wavelength tunable DBR lasers and widely tunable SGDBR lasers. His current research interests are in the development of integrated devices using lasers and semiconductor optical amplifiers.

Yongsoon Baek received the BS degree in physics from Seoul National University, Korea in 1991 and the PhD degree for research in nonlinear optics from CREOL at the University of Central Florida, US in 1997. From 1997 to 1998, he worked as a research associate at Washington State University. In 1999, he joined the Basic Communication Research Laboratory, ETRI, Korea where he has engaged in work on semiconductor optical amplifier related functional devices such as wavelength converters and space switches. Currently, he is working on the development of optical transceivers for passive optical networks.